Chapter 11
AI-Enhanced Anomaly Detection of Acoustic Emission Sensor Data via Clustering and Noise Discrimination: A Machine Learning-Based Study

Ali Bakhtiari, Tonghao Zhang, Antonio De Luca, and Nezar Abraham

Abstract Acoustic Emission (AE) monitoring has emerged as a powerful non-destructive testing (NDT) and structural health monitoring (SHM) technique for identifying early signs of damage in materials and structures. By capturing high-frequency stress waves generated by microcracking, fracture, or material deformation, AE provides unique insight into damage progression. However, AE data are often characterized by high volume, noise contamination, and complex feature distributions, making interpretation challenging. Artificial Intelligence (AI) and machine learning (ML) offer promising pathways for automating AE signal classification, anomaly detection, and real-time decision-making.

Within this study, a cantilever wood strip subjected to an increasing point load at its free end was monitored using AE sensors until failure. A total of 735 AE hits were collected and analyzed through a hybrid framework that combined unsupervised clustering with supervised classification. Five time-domain features were extracted, standardized, and reduced via principal component analysis (PCA) prior to k-means clustering. The analysis revealed two distinct clusters, corresponding to fracture-related burst events, and frictional noise from specimen–table interactions alongside minor secondary noise sources. Importantly, the frictional noise identified in this study differs from typical ambient noise, as its signal characteristics increase the likelihood of misclassification in AE-based SHM. Cluster validation using a k-nearest neighbor (K-NN) classifier achieved 98.3% accuracy, underscoring the robustness of the proposed methodology. The findings highlight the value of integrating clustering and supervised learning for reliable AE source discrimination. This work contributes to advancing SHM frameworks by demonstrating how challenging noise mechanisms can be identified and separated, thereby improving diagnostic reliability and applicability in real-time monitoring.

Keywords Acoustic emission · Unsupervised learning · Supervised learning · K-means clustering · Noise detection

Introduction

Acoustic Emission (AE) monitoring has become an increasingly important tool in non-destructive testing (NDT) and structural health monitoring (SHM) due to its ability to detect the initiation and progression of damage in real time [1]. AE signals are generated by transient stress waves released during events such as crack initiation, crack growth, fiber breakage, matrix cracking, or other localized deformations within materials [2]. Owing to its sensitivity and real-time capability, AE monitoring has been widely applied in aerospace, civil infrastructure, and mechanical systems to track the health of components and prevent catastrophic failures [3]. However, while AE provides a direct window into damage evolution, the technique is challenged by the complexity of the signals, which are often non-stationary, high-volume, and susceptible to noise contamination [4]. This complexity limits the reliability of conventional threshold-based or parametric interpretation methods, which frequently struggle to distinguish true damage events from irrelevant noise [5].

Ali Bakhtiari · Antonio De Luca
Thornton Tomasetti, Inc., 101 NE 3rd Ave #1170, Fort Lauderdale, FL 33301
e-mail: abakhtiari@thorntontomasetti.com; adeluca@thorntontomasetti.com

Tonghao Zhang · Nezar Abraham
Thornton Tomasetti, Inc., 600 W Fulton St, Suite 705, Chicago, IL 60661
e-mail: txzhang@thorntontomasetti.com; NAbraham@ThorntonTomasetti.com

Kristin B. Zimmerman, PhD (eds.), *Data Science in Engineering, 2026, Vol. 9*, Conference Proceedings of the Society for Experimental Mechanics Series, https://doi.org/10.1007/978-8-743-81448-1_11

Machine learning (ML) and artificial intelligence (AI) approaches have recently emerged as powerful solutions to address these challenges [6]. By leveraging feature extraction, clustering, and classification techniques, ML offers the capability to identify patterns in large AE datasets that are difficult to detect through traditional methods. Unsupervised learning methods, such as clustering, allow for grouping signals with similar feature characteristics, thereby enabling the identification of underlying physical mechanisms without requiring pre-labeled datasets. Meanwhile, supervised learning algorithms can be used to validate and refine these groupings, providing greater robustness for decision-making in SHM applications [7]. Several studies have successfully employed clustering methods, including *k*-means, hierarchical clustering, and density-based algorithms, to separate AE sources such as matrix cracking, fiber breakage, or delamination in composite materials [8]. Despite these advances, one persistent limitation is the treatment of noise. Ambient noise, operational vibrations, or frictional interactions are often overlooked or treated as background disturbances, even though their signal characteristics can overlap significantly with genuine AE events. Such misclassification can lead to inaccurate assessments of structural condition and false alarms in SHM systems.

The present study addresses this gap by focusing specifically on the identification and separation of friction-induced noise, which differs from typical ambient noise commonly reported in AE literature. The experimental dataset was obtained from a controlled test in which a cantilever wood strip resting on a testing table was subjected to an increasing point load at its free end until failure. During the experiment, 735 AE hits were recorded. These signals were analyzed through a hybrid machine learning framework combining *k*-means clustering with *k*-nearest neighbor (K-NN) classification. Five descriptive features were extracted from each AE hit, normalized, and reduced using principal component analysis (PCA) prior to clustering. The results revealed two distinct clusters, representing fracture-related burst signals, and frictional noise from specimen–table interactions alongside secondary minor noise sources. Notably, the frictional noise identified here exhibited waveforms that differed from ambient background noise but could closely resemble AE signals generated by damage, making it particularly prone to misclassification in both experimental and field monitoring applications. Validation using the supervised K-NN model achieved an accuracy of 98.3%, further demonstrating the robustness of the proposed approach.

This study contributes in two key ways. First, it demonstrates that unsupervised clustering combined with supervised validation provides a reliable means of distinguishing damage-related AE signals from noise, even in relatively small experimental datasets. Second, and more importantly, it highlights the significance of frictional noise as a distinct source of interference in AE monitoring, which has often been overlooked in prior studies. By explicitly identifying and separating this form of noise, the methodology enhances the reliability of AE-based diagnostics and provides a framework that can be extended to broader SHM and NDT applications. The findings underscore the importance of integrating machine learning approaches for anomaly detection in AE monitoring, while also recognizing that not all noise is ambient in origin, some may share signal characteristics with damage and thus demand careful classification.

Experimental Test Setup, Obtained Data, and AE Features

The experimental program was designed to generate acoustic emission (AE) signals during the failure of a wood strip specimen subjected to an increasing point load. The specimen was a rectangular wooden strip measuring 305 mm (12 in) in length, 102 mm (4 in) in width, and 3.2 mm (0.125 in) in thickness. It was positioned on a rigid testing table in a cantilever configuration, with an effective free length of 203 mm (8 in). A monotonic point load was applied at the free end of the strip using a loading fixture, and the magnitude of the load was gradually increased until fracture occurred at the fixed end. This simple test configuration was selected to promote crack initiation and failure under bending while minimizing boundary condition uncertainties.

AE activity was monitored throughout the loading process using a resonant R15α piezoelectric sensor manufactured by MISTRAS Group, Inc. The sensor was mounted on the strip at a distance of 76 mm (3 in) from the fixed end to maximize sensitivity to crack initiation and growth. The sensor was coupled to the specimen surface using a thin layer of silicone grease to ensure efficient acoustic transmission. The signal acquisition system was connected to the sensor via a preamplifier with a fixed gain setting, and waveforms were continuously recorded throughout the experiment. Figure 1 illustrates the experimental configuration, including the specimen geometry, loading setup, and AE acquisition system.

A total of 735 AE hits, or waveforms, were captured during the loading and failure process. Each AE hit corresponds to a transient elastic wave detected by the sensor when a micro-event occurs within the specimen or at the specimen–table interface. From each recorded waveform, five standard AE features were extracted: rise time, hit counts, signal energy, duration, and amplitude. These features were selected due to their proven relevance for AE characterization in prior NDT and SHM studies. Rise time provides information on the signal onset and sharpness, hit counts reflect the number of threshold crossings within a waveform, energy quantifies the cumulative signal strength, duration measures the time span of the signal above threshold, and amplitude represents the maximum signal intensity. Together, these descriptors provide a balanced characterization of AE signals in both time and intensity domains, forming the input feature set for subsequent machine learning analysis.

(a) (b)

Fig. 1 The experimental setup and data acquisition system: (a) Before applying the increasing point load at the free end, and (b) After breakage/failure of the wood strip specimen

Anomaly/Damage Identification via Machine Learning

The differentiation of acoustic emission (AE) sources that exhibit distinct signal characteristics, such as rise time, frequency centroid, and peak frequency, represents a fundamental step toward identifying the physical mechanisms responsible for material damage. Clustering analysis provides a robust framework for this task by grouping signals with comparable feature attributes, thereby enabling the separation of genuine damage events from spurious sources such as environmental noise or frictional interactions.

Among the available clustering techniques, the *k*-means algorithm remains one of the most widely employed due to its computational efficiency, scalability, and methodological simplicity. The algorithm partitions a dataset into *k* non-overlapping groups by iteratively assigning each observation to the nearest centroid and subsequently updating centroid positions until convergence is achieved. This iterative process ensures a balance between intra-cluster similarity and inter-cluster separation, making *k*-means particularly suitable for large, high-dimensional AE datasets.

In the present study, *k*-means clustering was implemented to fingerprint AE sources and to classify recorded signals into representative groups associated with two dominant mechanisms: (i) frictional noise caused by specimen–support interactions and (ii) fracture processes leading to wood panel failure. The procedure was first applied to the experimental training dataset to establish baseline AE classes, and the resulting clusters were then validated using a supervised *k*-nearest neighbors (KNN) approach, thereby providing an independent check on classification reliability.

Prior to clustering, the AE signals underwent a structured three-stage preprocessing pipeline. First, five descriptive features, counts, energy, rise time, amplitude, and duration, were extracted for each hit to capture essential time-domain characteristics. Second, all extracted features were standardized to unit variance. This normalization step mitigates disparities arising from heterogeneous physical units and ensures balanced feature contributions during clustering, while also aligning with best practices for preparing data for principal component analysis (PCA). Finally, dimensionality reduction was performed using PCA to facilitate visualization and suppress noise. Four principal components, explaining more than 90% of the cumulative variance, were retained for further analysis, as shown in Figure 2.

The number of clusters was determined using the silhouette coefficient, a well-established metric for evaluating the quality of unsupervised partitions. For each data point, the silhouette value is defined as (b-a)/max (a, b), where a denotes the average intra-cluster distance and b the minimum average distance to the nearest external cluster. The coefficient ranges between -1 and 1, with values closer to 1 indicating strong cohesion within clusters and good separation between clusters. As shown in Figure 3, the silhouette analysis revealed that 2 clusters provided the optimal balance of cohesion and separation, thereby representing the most suitable configuration for the dataset.

While Table 1 summarizes the sample size distribution across the identified clusters, the visualization of the k-means clustering results is presented in Figure 4. The figure displays the AE hits in the reduced principal component (PCA) space, where distinct groupings are clearly observable. The clustering procedure successfully partitioned the dataset into sepa-

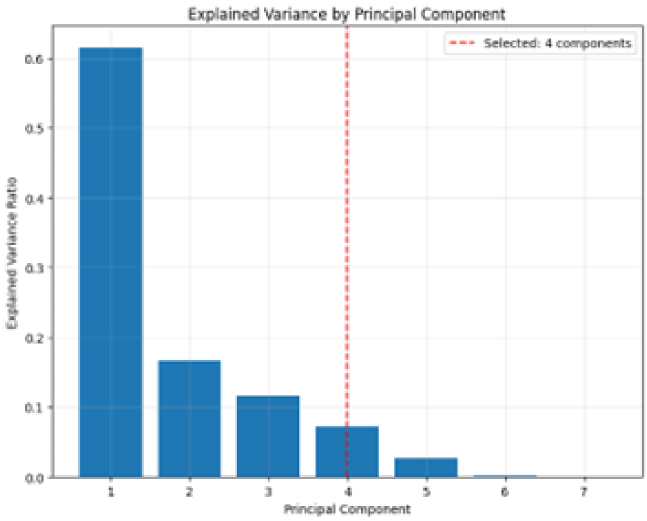

(a)

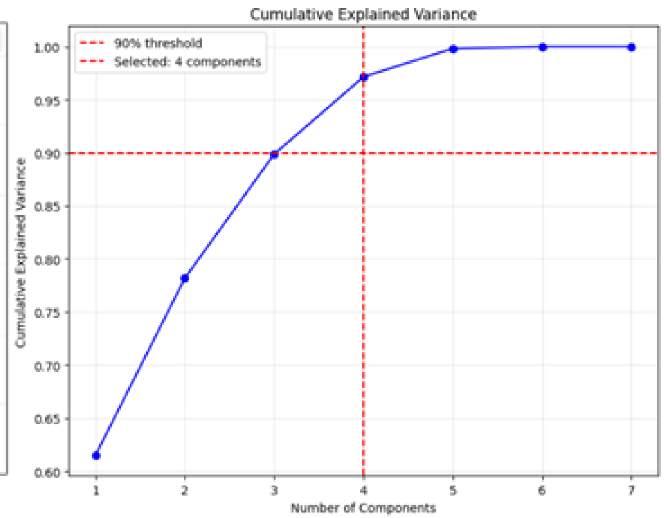

(b)

Fig. 2 PCA Analysis: Four principal components explaining more than 90% of the cumulative variance were retained for further analysis

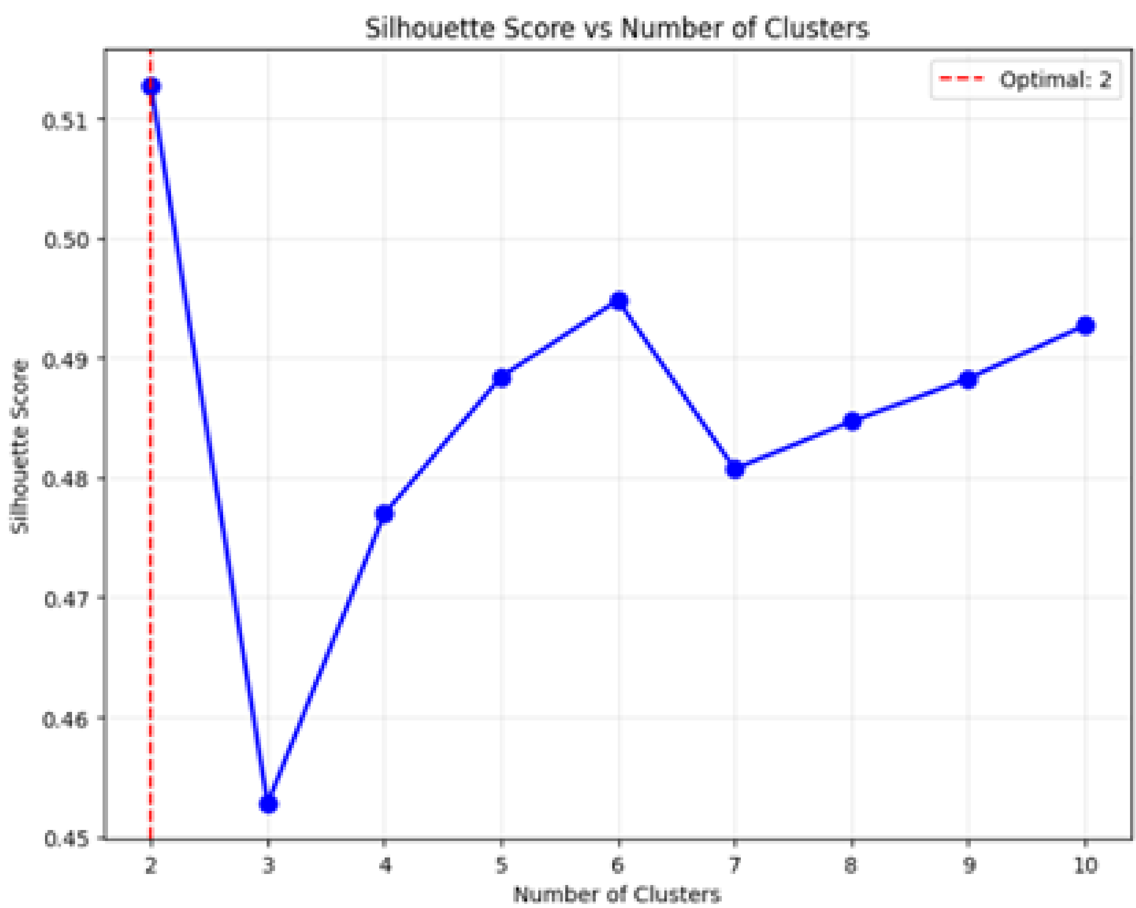

Fig. 3 Optimum number of clusters based on the Silhouette Score

rate clusters, demonstrating its ability to discriminate between signal types based on their extracted features. In particular, two dominant clusters emerged with minimal overlap, indicating that the feature set and dimensionality reduction strategy

Table 1 Number of clusters with their corresponding size distribution and percentage of samples

Cluster	Cluster Size Distribution	Percentage
0	626 Samples	85.2 %
1	109 Samples	14.8 %

provided sufficient discriminatory power to separate AE events associated with different underlying mechanisms. The well-defined grouping observed in Figure 4 confirms the robustness of the unsupervised learning approach in identifying patterns within the AE dataset without requiring prior labeling. This outcome not only validates the suitability of k-means for handling AE signals but also provides the foundation for further interpretation of the clusters in relation to fracture-induced signals and noise-related events. These results confirm that clustering, supported by careful feature engineering and dimensionality reduction, offers a viable and effective means of distinguishing between frictional noise and true fracture events in AE monitoring of wood panel failure.

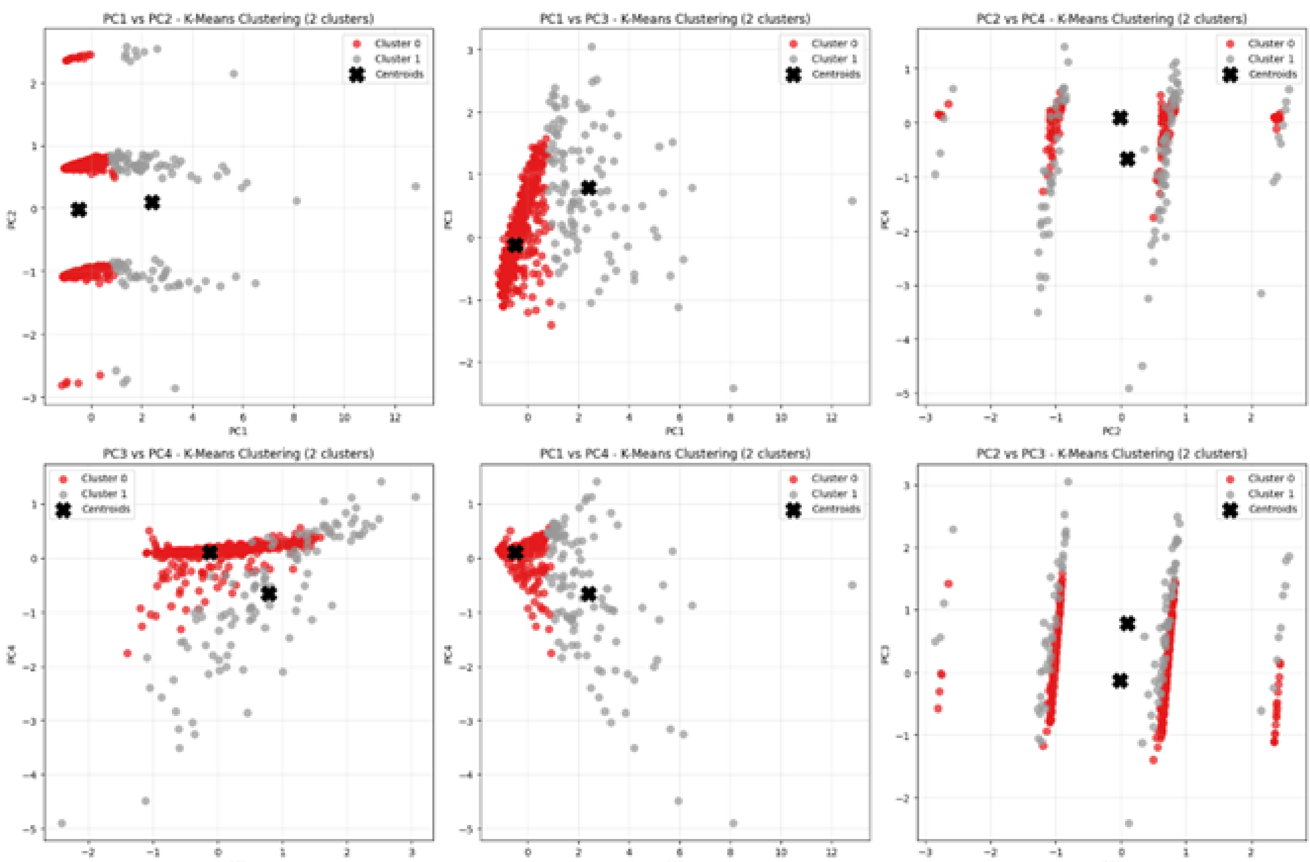

Fig. 4 2-D visualization of the k-means clustering results in the reduced principal component (PCA) space

As illustrated in Figure 5, representative waveforms corresponding to Cluster 0 and Cluster 1 are presented to demonstrate the distinct temporal characteristics of each class. Clear differences in waveform morphology are evident. The waveform associated with Cluster 0, attributed to AE hits generated during the wood strip failure, exhibits a burst-type profile, characterized by a rapid initial rise followed by a sudden attenuation. This sharp, transient form is consistent with the expected signature of fracture-related AE events, where the release of strain energy occurs abruptly as microcracks initiate and propagate.

In contrast, the representative waveform from Cluster 1 displays no such burst-type morphology. Instead, it reveals a more irregular and less impulsive shape, which is indicative of frictional noise. This type of signal is associated with the sliding movement of the specimen across the testing table and the frictional interactions between the two contact surfaces. The

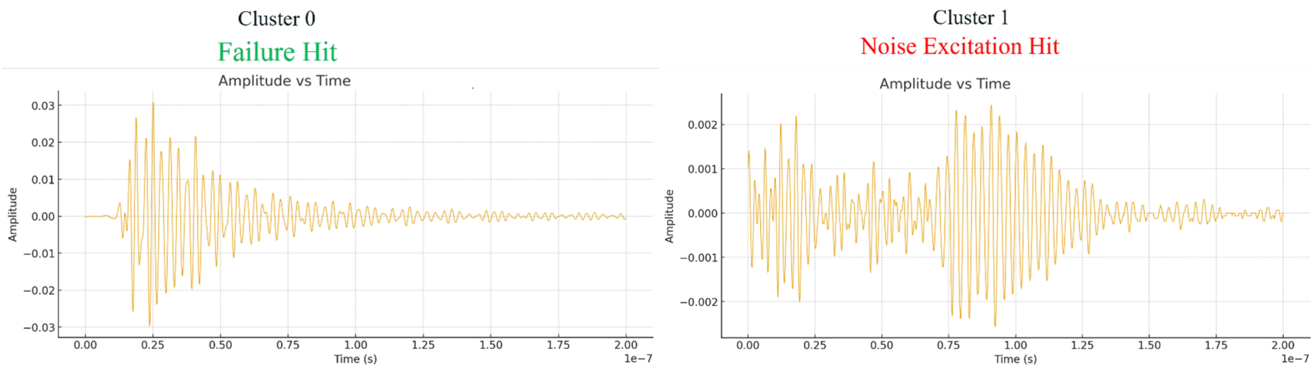

(a) (b)

Fig. 5 Comparison between the two waveforms: Failure Hit vs Noise Excitation Hit

absence of a sharp onset and the presence of extended fluctuations suggest a fundamentally different physical mechanism compared to Cluster 0. Moreover, the maximum amplitude of the AE hit associated with wood strip failure (Cluster 0) was found to be approximately 15 times greater than that of the representative noise waveform (Cluster 1). This pronounced difference in signal intensity provides additional evidence supporting the distinction between the two classes. High-amplitude burst-type signals are generally characteristic of fracture events, where the sudden release of elastic energy produces sharp transients detectable by AE sensors. In contrast, noise-related signals generated by frictional sliding or surface interactions typically exhibit lower amplitudes due to their more gradual and distributed energy release. The observed amplitude disparity therefore, reinforces the interpretation that the clustering algorithm successfully differentiates true failure-related AE events from background noise.

The ability of the clustering procedure to segregate these signal types underscores its effectiveness in distinguishing fracture-induced AE hits from noise-related events. By isolating bursts associated with material failure from frictional artifacts, the method enhances the reliability of AE monitoring for structural diagnostics and provides a more accurate interpretation of the underlying physical processes.

Figure 6 presents the hit rate histograms for all AE signals categorized within each cluster. A clear distinction in event frequency is observed between the two groups. Specifically, the mean hit rate of Cluster 0, corresponding to specimen failure events, is approximately 5.7 times greater than that of Cluster 1, which is associated with frictional noise, sustained over the entire duration of the experiment. This elevated hit rate for Cluster 0 is consistent with the expected increase in AE activity during progressive damage accumulation and eventual structural failure. In contrast, the comparatively lower rate of Cluster 1 indicates that noise-related events occur less frequently and do not dominate the monitoring record. The pronounced difference in event occurrence between the two clusters further validates the ability of the applied clustering framework to isolate genuine fracture-related activity from extraneous noise sources, thereby enhancing the reliability of AE-based diagnostics.

To further evaluate the relationship between the identified clusters and their corresponding AE sources, as well as to assess the robustness of the clustering model, a supervised classification approach was employed using the *k*-nearest neighbor (K-NN) algorithm. The dataset was partitioned evenly into training and testing subsets, and the dissimilarity between data points was quantified using the Euclidean distance metric. Euclidean distance was selected due to its low computational cost, which is particularly advantageous for real-time monitoring applications where large volumes of AE data are continuously collected. The preprocessing steps, including unit variance scaling and principal component analysis (PCA) for dimensionality reduction, further enhanced the performance of the K-NN model by ensuring balanced feature contributions and mitigating the risk of overfitting in high-dimensional space.

To determine the optimal number of neighbors, multiple values were systematically evaluated. The results indicated that selecting three neighbors yielded the highest classification accuracy, achieving 98.3%. Conversely, increasing the number of neighbors to five reduced performance by introducing misclassifications, while using a single neighbor resulted in susceptibility to outliers and decreased robustness. Therefore, three neighbors were adopted as the optimal configuration for the K-NN model in this study.

The model's predictive accuracy was validated by comparing predicted labels with the actual cluster assignments, as shown in Figure 7. The confusion matrix reveals that the vast majority of AE signals were classified correctly into their respective clusters, with only minimal misclassification observed in off-diagonal entries. These findings confirm that the

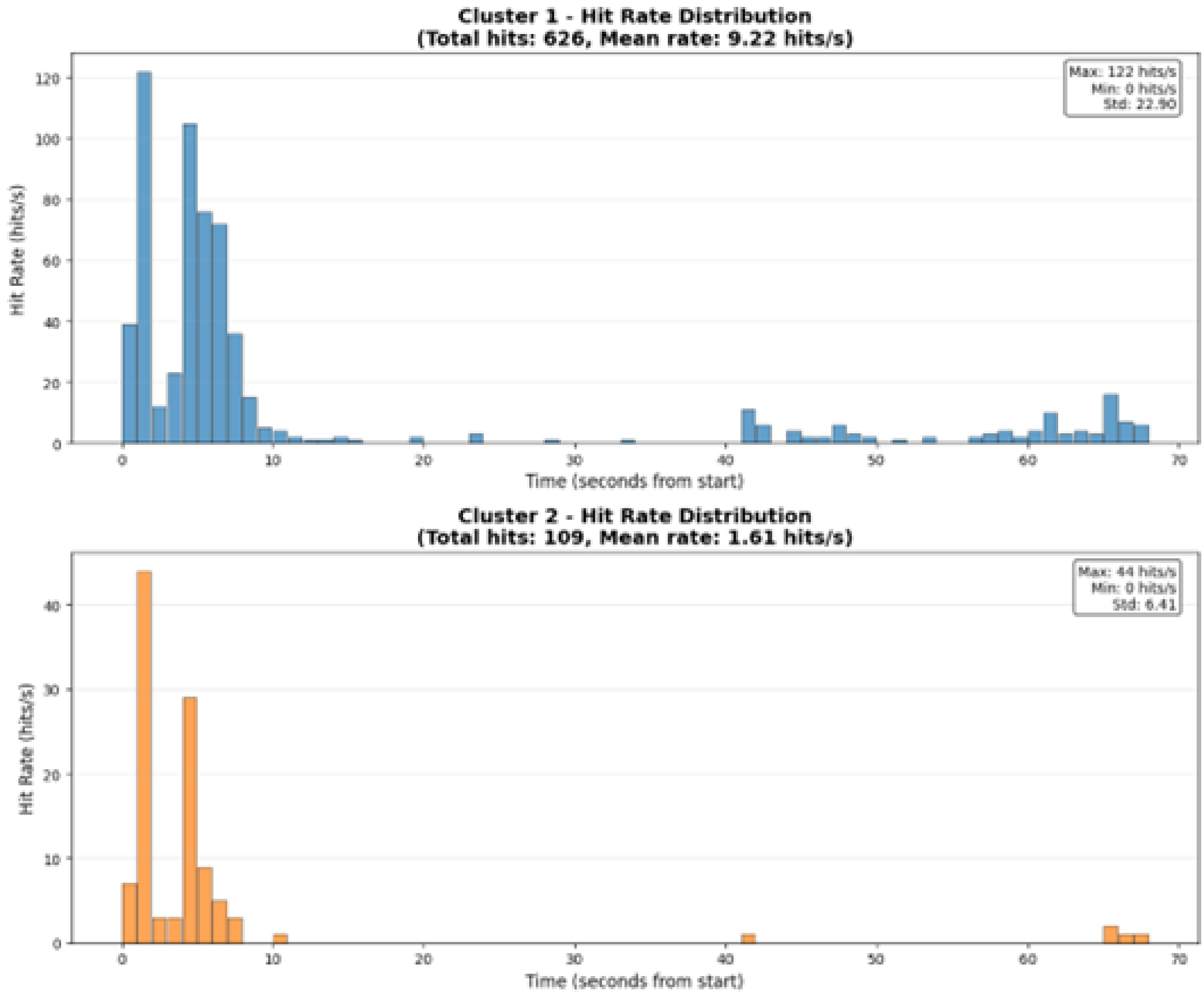

Fig. 6 Hit rate histograms for Cluster 0, corresponding to the specimen's failure, and Cluster 1, associated with frictional noise

supervised K-NN model effectively corroborates the outcomes of the unsupervised clustering, thereby reinforcing confidence in the separation of fracture-related AE events from noise-induced signals.

Figure 8 illustrates the comparison between the true cluster labels of the test set (left) and the predicted labels generated by the K-NN classifier (right). In both plots, the data are visualized in the reduced PCA space, with PC1 and PC2 serving as the horizontal and vertical axes, respectively. The left panel shows the true labels of AE hits in the test set, where three distinct bands corresponding to the identified clusters are visible. These bands reflect the underlying separability of AE signals into meaningful groups associated with fracture-related events and noise sources. The right panel presents the predicted labels obtained using the K-NN model with three neighbors. Correct classifications are denoted by gray points, while misclassified instances are marked with red crosses. The overall prediction accuracy reached 98.3%, with only a small number of data points located near the cluster boundaries being misclassified. This outcome is expected, as boundary regions typically exhibit overlapping feature characteristics, making them more difficult to distinguish with high certainty.

The close correspondence between the predicted and true label distributions demonstrates the robustness of the K-NN model in validating the unsupervised clustering results. The high classification accuracy further supports the conclusion that the applied preprocessing, dimensionality reduction, and optimal neighbor selection collectively contributed to the model's performance. Importantly, the small fraction of misclassified signals does not alter the overall interpretation of the clustering outcome, as the vast majority of AE hits were accurately assigned to their respective groups.

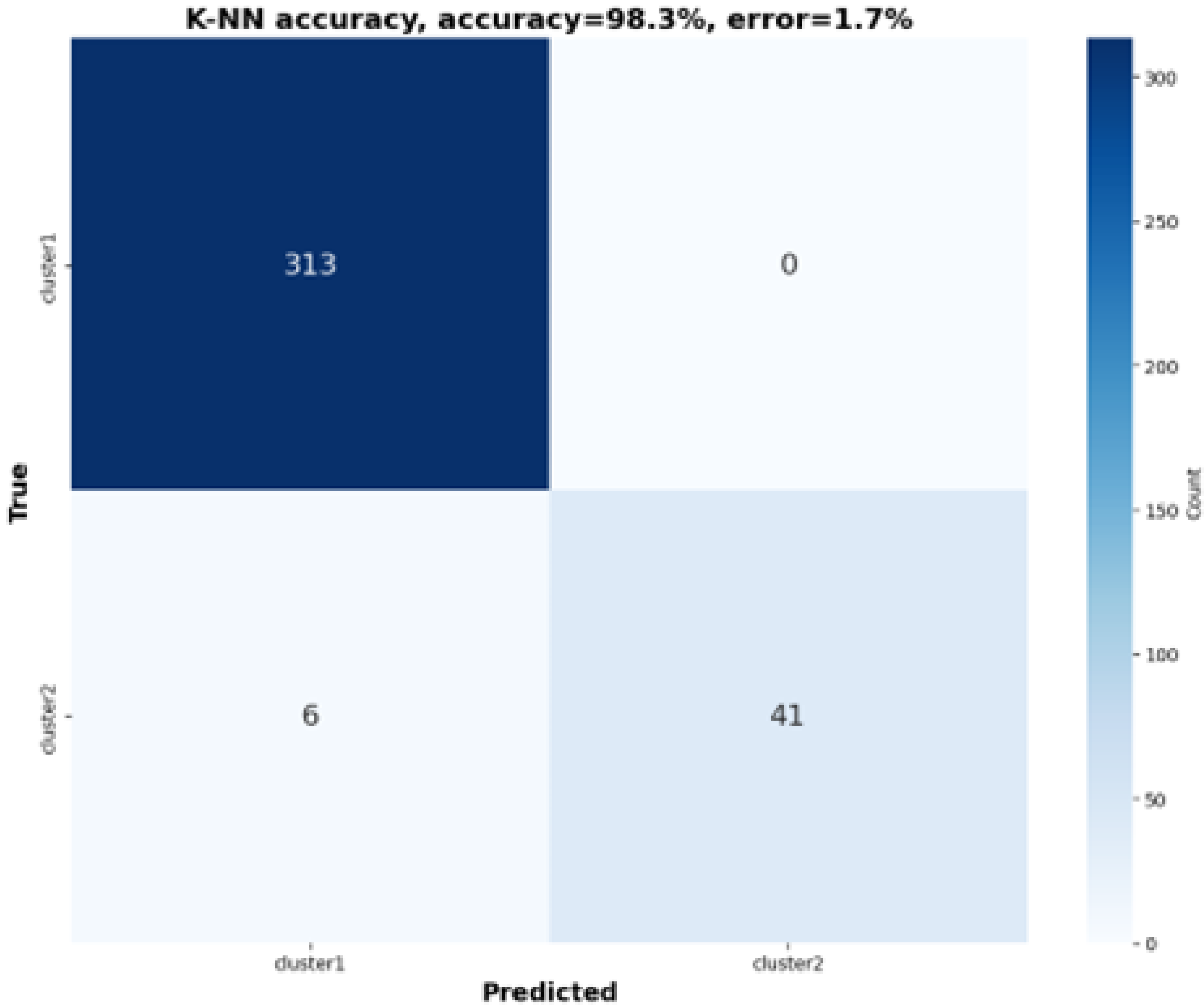

Fig. 7 Confusion matrix for K-NN results showing a prediction accuracy of 98.3 %

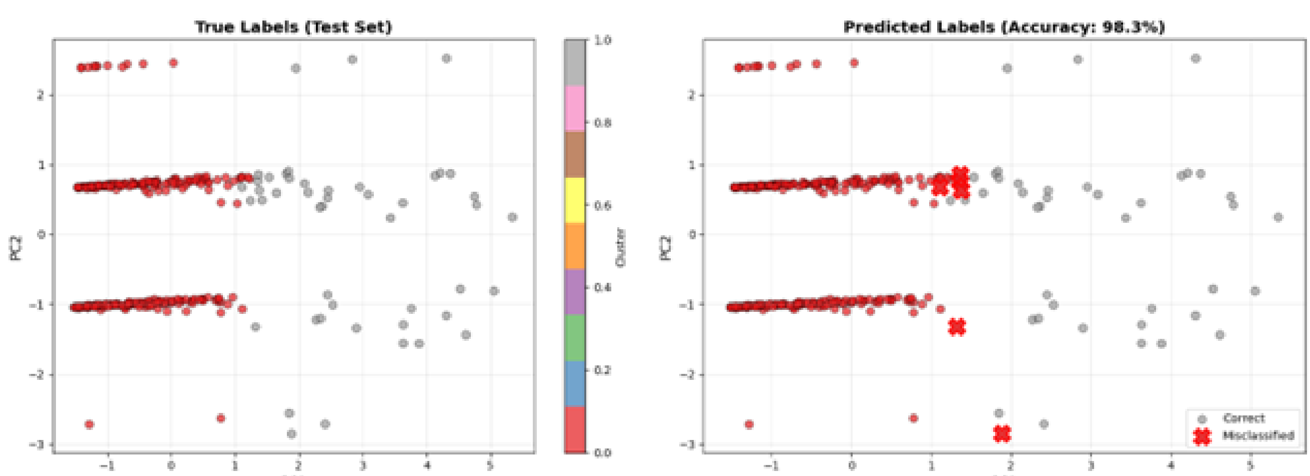

Fig. 8 The comparison between the true cluster labels of the test set (left) and the predicted labels generated by the K-NN classifier (right)

Conclusions

This study investigated the classification of acoustic emission (AE) signals collected during the failure of a cantilever wood strip subjected to an increasing point load at its free end. A total of 735 AE hits were recorded throughout the experiment and systematically analyzed using an unsupervised–supervised hybrid framework combining *k*-means clustering and *k*-nearest neighbor (K-NN) classification. The objective was to distinguish between genuine fracture-induced AE events and noise signals associated with specimen–table interactions. The findings demonstrate that clustering analysis, supported by feature extraction, normalization, and dimensionality reduction, provides an effective means of isolating distinct AE sources. The *k*-means algorithm successfully partitioned the dataset into three clusters, which were subsequently interpreted as (i) fracture-related burst signals, (ii) frictional noise generated by the sliding of the specimen on the table, and potentially minor noise sources. Morphological differences between representative waveforms confirmed the separation, with fracture events exhibiting sharp burst-type profiles and significantly higher amplitudes compared to frictional signals. Quantitatively, the failure-related AE hits showed maximum amplitudes approximately 15 times higher and mean hit rates 5.7 times greater than their noise counterparts, reflecting the dominant role of fracture processes during structural failure. Importantly, the type of noise identified in this study is distinct from typical ambient noise often considered in AE monitoring. Instead of arising from environmental disturbances, the identified noise originated from friction between the specimen and the testing table. This type of frictional noise is particularly challenging, as it shares certain signal characteristics with genuine AE events and therefore has a higher likelihood of being misclassified in similar studies or structural health monitoring (SHM) applications. By explicitly identifying and separating this noise mechanism, the present study contributes to advancing the reliability of AE data interpretation in experimental and field contexts. Validation using the supervised K-NN classifier yielded an accuracy of 98.3%, further confirming the robustness of the clustering approach. Only a limited number of misclassifications were observed, primarily in boundary regions where feature overlap between clusters is expected. Overall, the results confirm that the combination of clustering and supervised validation provides a reliable framework for distinguishing fracture-induced AE activity from noise in experimental testing. Beyond this case study, the proposed methodology has broader applicability to SHM and nondestructive testing, where accurate separation of damage signals from background noise is essential for diagnostic reliability. Future work will focus on extending the approach to larger and more heterogeneous datasets, incorporating additional frequency-domain features, and exploring advanced machine learning classifiers to further enhance real-time AE source discrimination.

Acknowledgments The authors gratefully acknowledge the support of Thornton Tomasetti's Core Lab, whose funding and resources made this study possible. Their commitment to advancing innovation in structural engineering and applied research provided the foundation for the successful completion of this work.

References

1. Melchiorre, Jonathan, et al. "Acoustic emission and artificial intelligence procedure for crack source localization." Sensors 23.2 (2023): 693.
2. Zhang, Tonghao, Chenxi Xu, and Didem Ozevin. "Acoustic emission source localization in complex pipe structure using multi-task deep learning models." Advances in Structural Engineering 28.1 (2025): 23-37.
3. Ahmed, Junaid, et al. "A multiscale indentation-based technique to correlate acoustic emission with deformation mechanisms in complex alloys." *Materials Characterization* 182 (2021): 111575.
4. Tagawa, Y., R. Maskeliunas, and R. Damaševicius. "Acoustic Anomaly Detection of Mechanical Failures in Noisy Real-Life Factory Environments. Electronics 2021, 10, 2329." 2021,
5. König, F., et al. "Machine learning based anomaly detection and classification of acoustic emission events for wear monitoring in sliding bearing systems." *Tribology International* 155 (2021): 106811.
6. Thirumalaiselvi, A., and Saptarshi Sasmal. "Machine learning-based acoustic emission technique for corrosion-induced damage monitoring in reinforced concrete structures." *Engineering Applications of Artificial Intelligence* 137 (2024): 109121.
7. Vos, Kilian, et al. "Vibration-based anomaly detection using LSTM/SVM approaches." *Mechanical Systems and Signal Processing* 169 (2022): 108752.
8. Zhang, Tonghao, et al. "Experimental study on monitoring damage progression of basalt-FRP reinforced concrete slabs using acoustic emission and machine learning." *Sensors* 23.20 (2023): 8356.